

NASTaR: NovaSAR Automated Ship Target Recognition Dataset

Benyamin Hosseiny, *Member, IEEE*, Kamirul Kamirul, Odysseas Pappas, and Alin Achim, *Senior Member, IEEE*

Abstract—Synthetic Aperture Radar (SAR) offers a unique capability for all-weather, space-based maritime activity monitoring by capturing and imaging strong reflections from ships at sea. A well-defined challenge in this domain is ship type classification. Due to the high diversity and complexity of ship types, accurate recognition is difficult and typically requires specialized deep learning models. These models, however, depend on large, high-quality ground-truth datasets to achieve robust performance and generalization. Furthermore, the growing variety of SAR satellites operating at different frequencies and spatial resolutions has amplified the need for more annotated datasets to enhance model accuracy. To address this, we present the NovaSAR Automated Ship Target Recognition (NASTaR) dataset. This dataset comprises of 3415 ship patches extracted from NovaSAR S-band imagery, with labels matched to AIS data. It includes distinctive features such as 23 unique classes, inshore/offshore separation, and an auxiliary wake dataset for patches where ship wakes are visible. We validated the dataset’s applicability across prominent ship-type classification scenarios using benchmark deep learning models. Results demonstrate over 60% accuracy for classifying four major ship types, over 70% for a three-class scenario, more than 75% for distinguishing cargo from tanker ships, and over 87% for identifying fishing vessels. The NASTaR dataset is available at <https://10.5523/bris>, while relevant codes for benchmarking and analysis are available at <https://github.com/benyaminhosseiny/nastar>.

Index Terms—SAR dataset, Ship ATR, NovaSAR, maritime surveillance.

I. INTRODUCTION

SYNTHETIC Aperture Radar (SAR) is a coherent imaging technique capable of high-resolution imaging regardless of weather or lighting conditions. Unlike optical sensors, SAR ability to operate in day-and-night scenarios and penetrate cloud cover makes it indispensable for maritime monitoring tasks such as ship detection, classification, and tracking [1].

SAR systems operate across various frequency bands, such as X, C, L, and more recently, the S-band, each offering distinct trade-offs. Higher-frequency bands (e.g., X and C bands) provide finer spatial resolution, enabling detailed object delineation but suffer from limited penetration and lower SNR in cluttered environments. Lower-frequency bands (e.g., the

The authors are with the Visual Information Laboratory, University of Bristol, BS1 5DD Bristol, U.K. (e-mail: ben.hosseiny@bristol.ac.uk; kamirul.kamirul@bristol.ac.uk; o.pappas@bristol.ac.uk; alin.achim@bristol.ac.uk)

This work was supported in part by the Engineering and Physical Sciences Research Council under Grant EP/X525674/1 EPSRC Impact Acceleration Account - University of Bristol 2022 and in part by the Dstl under the DASA Defence Rapid Impact Open Call. The work of Kamirul Kamirul was supported by Lembaga Pengelola Dana Pendidikan (LPDP), Ministry of Finance of the Republic of Indonesia.

L-band) offer deeper penetration and broader swath coverage, but at the cost of reduced spatial resolution. S-band SAR, exemplified by platforms like NovaSAR and NiSAR, offers a compromise between resolution and coverage. Its moderate wavelength allows for improved SNR and wider swath acquisition compared to the X- and C bands, while retaining sufficient resolution for object-level analysis [2]. These characteristics make S-band SAR particularly promising for large-scale maritime surveillance, where both spatial detail and temporal coverage are critical.

SAR imagery is fundamentally different from optical imagery due to its coherent nature and side-looking geometry. Key phenomena such as speckle noise, layover, foreshortening, and shadowing complicate interpretation. In addition, the backscattering response of maritime targets is influenced by factors such as hull geometry, surface roughness, and sea state, leading to highly variable target signatures. These complexities pose significant challenges for automatic target recognition (ATR) in SAR imagery. Traditional approaches based on physical scattering models or handcrafted features often fail to generalize across varying acquisition conditions and target types [3].

Deep learning (DL) has become a key approach for SAR-based ATR, enabling end-to-end learning that jointly optimizes feature extraction and tasks like detection and classification. DL models capture complex spatial patterns through hierarchical representations and nonlinear transformations, eliminating manual feature engineering. A variety of DL architectures have demonstrated state-of-the-art performance in SAR target detection, classification, and segmentation, and can run on GPUs for real-time inference. However, while their success depends on large, high-quality annotated datasets, achieving it is challenging due to expert interpretation requirements and radar signature ambiguity.

Benchmark datasets play a critical role in advancing DL research by providing standardized evaluation protocols and facilitating reproducibility. While several SAR datasets exist for ship detection and classification, most are based on X- or C-band imagery and focus on binary detection or coarse classification tasks [4]. There is a notable gap in publicly available datasets tailored to S-band SAR imagery, especially for fine-grained ship-type classification. Given the unique imaging characteristics of the S-band and its growing adoption in maritime surveillance, a dedicated benchmark is essential to support model development, cross-band generalization studies, and operational deployment.

In this paper, we introduce NASTaR (NovaSAR Automated Ship Target Recognition), a benchmark dataset for ship-

type classification in S-band SAR images acquired from the NovaSAR satellite. The dataset includes annotated samples across multiple ship categories, enabling tasks that include (i) ship detection and classification: distinguishing between fishing, cargo, tanker, and other vessel types; (ii) wake identification: recognizing ship wakes and their patterns for ship classification and motion inference; (iii) model benchmarking: evaluation of the performance of various DL architectures for S-band SAR imagery.

The remainder of this paper is organized as follows. Section II reviews public ship recognition datasets from SAR imagery and related state-of-the-art analysis techniques. Section III describes the construction of NASTaR, its key features, and statistical insights, including class distributions and variations in object shapes and orientations. Section IV presents benchmark results, evaluating deep learning models on the NASTaR dataset, with concluding remarks in Section V.

II. RELATED WORKS

A. Existing SAR Ship Recognition Datasets

Publicly available datasets for ship ATR using SAR imagery remain limited. One of the earliest is the HR-SAR dataset [5], released in 2013, comprising 450 high-resolution (2×1.5 m, X-band) TerraSAR-X images across three ship categories. Another widely used resource is OpenSARShip [6], [7]. Derived from Sentinel-1 data in SLC and GRD formats, under VH and VV polarizations. A key limitation of this dataset is significant class imbalance, which hampers classification robustness and generalization. xView3-SAR [8] is another dataset focused on detecting dark vessels, making it suitable for identifying illegal activities using Sentinel-1 GRD imagery. Other notable datasets originate from the Gaofen satellite series, known for their high spatial resolution and detailed backscattering. Examples include FUSAR [9] and MTCD [10]. Note that none of the above datasets include S-band SAR imagery.

Although ship wake patterns are useful for identifying smaller vessels that are difficult to detect in low-resolution SAR imagery, datasets dedicated to wake detection and identification remain extremely limited. Most existing datasets concentrate on wake detection, rather than classification. For instance, OpenSARWake [11] supports wake detection tasks and includes samples from Sentinel-1, Gaofen, and ALOS-PALSAR satellites. However, to the best of our knowledge, there is no publicly available dataset specifically designed for ship identification based on wake patterns. The only notable exception is SynthWakeSAR [12], which simulates SAR images of ship wakes based on hydrological modeling of the sea surface.

B. Deep learning Techniques in Ship Target Recognition

Recent research efforts have been undertaken to improve SAR ship ATR by addressing main challenges, such as class imbalance, noisy, varied shapes, and sparse backscattering. For example, to mitigate the class imbalance problem in the FUSAR and OpenSARShip datasets, Zhang et al., [13] proposed a lightweight customized CNN model and a training process based on identifying the center of each class in the

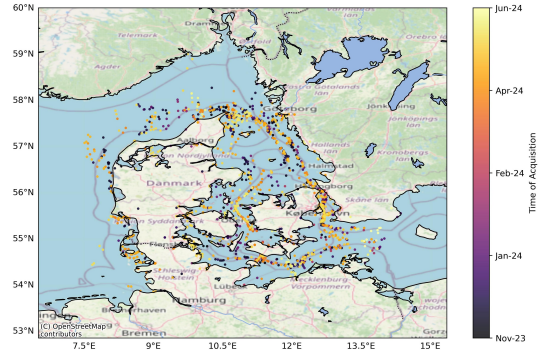


Fig. 1. Geographic and temporal distribution of the constructed dataset

deep feature space, followed by gradually balanced sampling. To address the large shape and size variations among different ship types and the significant inter-class overlap, a multiscale feature attention mechanism was introduced in [14]. This approach improved classification accuracy through an adaptive weighting technique that effectively emphasizes features from different scales. To enhance model robustness and reliability in ship recognition, Zheng et al., [15] developed a MetaBoost-based ensemble learning model, which demonstrated improved performance across diverse SAR scenes.

III. THE NASTAR DATASET

NovaSAR was launched in 2018 and aims to demonstrate the potential of low-cost, miniature SAR satellites for maritime monitoring and land use applications. It is an S-band (3.2 GHz) satellite producing medium resolution (6-30m) images. To construct NASTaR, 624 NovaSAR images captured over the North sea and the Danish straits between November 2023 and June 2024 were used. The images were acquired in Stripmap mode with 6m resolution and are ground-range detected (GRD). The temporal and spatial distribution of ship presence during this period is illustrated in Fig. 1.

Coupling the image with ground truth AIS data is a key element of NASTaR. The NovaSAR satellite carries its own AIS instrument, meant to provide complementary ship tracking data for maritime monitoring applications. Here, however, we have opted to correlate the ships in the SAR images with AIS data provided by the Danish Maritime Authority [16] as their ground-based AIS transponders covering our area of interest are more accurate and capable of reliably capturing signals from dense ship populations. The AIS samples were filtered to the same geographical zone as the corresponding SAR scene and within a 5-minute time window around the acquisition time. In addition to the ship's location and timestamp, the AIS dataset includes information such as speed over ground (SOG), heading angle, and vessel type and dimensions.

Each ship patch sample is generated by mapping the latitude and longitude from the AIS data to the corresponding location in the NovaSAR image. The patches are sized at 512x512 pixels, equivalent to 1280x1280 m² on the ground. Initially, 3415 ship patches were extracted. To classify these patches as either inshore or offshore, the distance from the ship's location to the nearest landmass was calculated using Natural

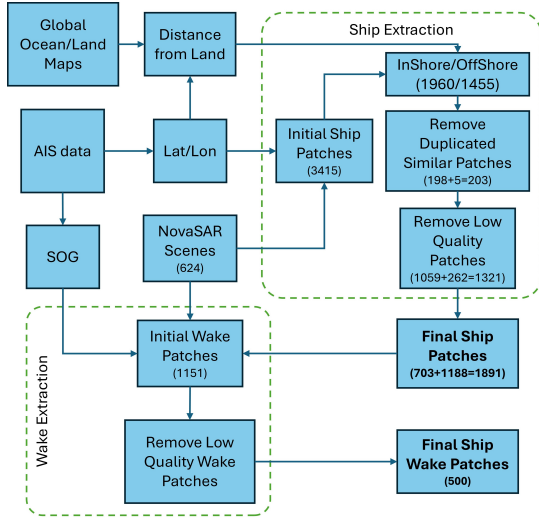


Fig. 2. Block diagram of the semi-automated patch extraction pipeline.

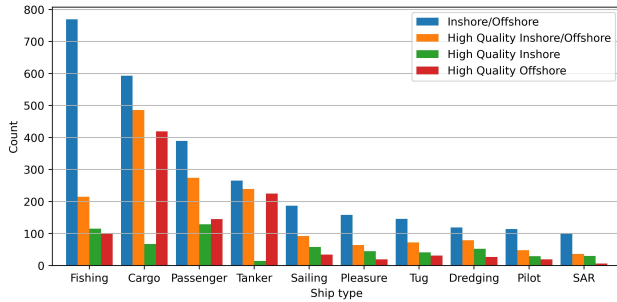


Fig. 3. Class distribution of the extracted ship images.

Earth maps [17]. A threshold of 500 meters was used to distinguish between inshore and offshore patches, resulting in 1960 inshore and 1455 offshore patches. The calculated distance to shore per sample is provided so as to enable users to define custom inshore/offshore splits as needed.

Two data filtering steps were applied: one to remove duplicate patches where multiple ships were located close together, and another to eliminate low-quality patches with excessive noise or unclear ship patterns. As a result, 198 inshore and 5 offshore duplicate patches were removed, along with 1059 inshore and 262 offshore low-quality patches. The final dataset consists of 1891 ship patches, including 703 inshore and 1188 offshore samples. To extract ship wake samples, AIS-derived SOG data was used to identify ships moving faster than 1 m/s, which are likely to generate visible wake patterns. Initially, 1151 wake candidate patches were extracted. After filtering out low-quality samples (where wake visibility was poor due to a number of factors including sea state and SAR viewing geometry), 500 wake patches were retained. Each wake patch is sized at 1024×1024 pixels (2560×2560 m² on the ground), with the ship positioned in a corner rather than the center to better capture the extended wake pattern. The flowchart of semi-automated extraction and labeling of ship and ship wake patches is shown in Fig. 2.

The complete extracted dataset comprises over 23 distinct

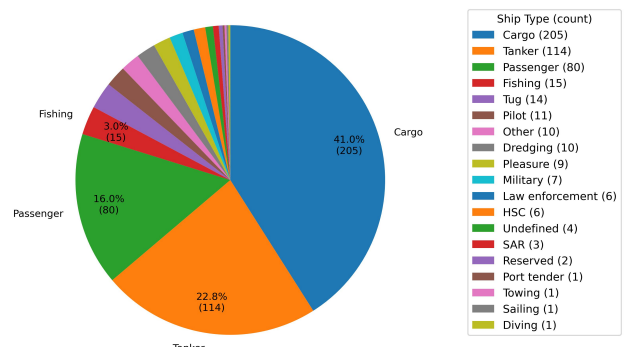


Fig. 4. Corresponding class distribution of extracted ship wakes.

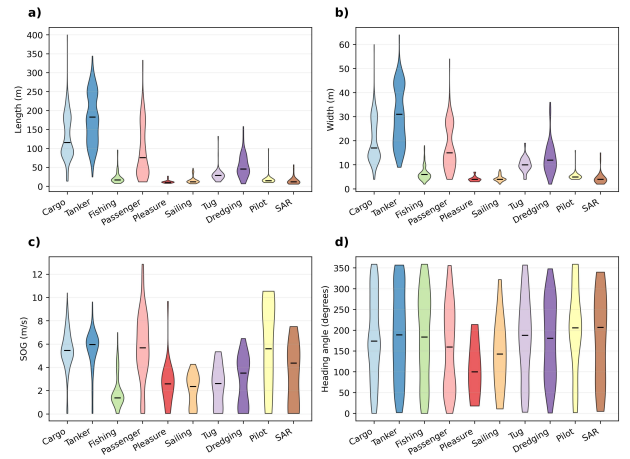


Fig. 5. Statistical distribution of ship characteristics: a) Length, b) Width, c) SOG, d) Heading angle

ship types, including cargo, tanker, fishing, passenger, and sailing vessels. Fig. 3 shows the distribution of the top 10 ship types in the dataset. Fishing vessels are the most prevalent in the initial dataset, while cargo ships dominate after filtering, particularly in offshore regions. Cargo ships also constitute the majority of samples in the ship wake dataset, followed by tanker and passenger ships (Fig. 4).

Fig. 5 provides statistical information on ship shapes and movement behavior derived from AIS data, including length, width, speed over ground (SOG), and heading angle. The heading angle represents the direction of the vessel relative to true north, ranging from 0° to 360°. From this figure, it is evident that the dataset contains a wide variety of ship shapes across different types. For instance, there is a significant range and overlap in the length and width of Cargo, Tanker, and Passenger ships. Cargo ships exhibit the broadest range of lengths and widths, whereas Tankers have the highest average length and width among all categories.

IV. BENCHMARK EXPERIMENTS

To validate and analyze the dataset, we explored several classification scenarios commonly examined in the literature. We focused on four primary ship types: Cargo, Tanker, Fishing, and Passenger. Cargo ships are versatile vessels designed to transport goods and materials across oceans and seas,

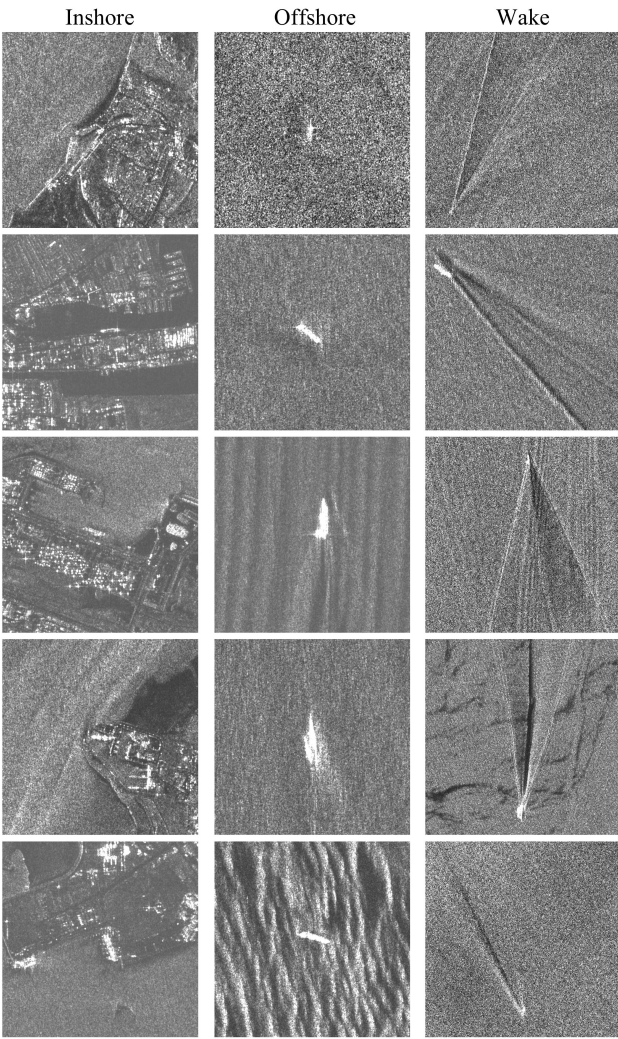


Fig. 6. Samples from NASTaR: From top to bottom, each row corresponds to fishing boats, cargo, tanker, passenger, and tug, respectively.

playing a vital role in global trade. Tankers are specialized ships built to carry bulk liquid cargo, such as crude oil, chemicals, and liquefied natural gas, making them indispensable to the energy and chemical industries. Cargo and tanker ships share several structural and operational similarities, including large hull sizes, similar radar signatures, and standardized navigation patterns. Differentiating between these vessel types is crucial for accurate maritime domain awareness, particularly in regions with high traffic or sensitive geopolitical contexts. However, these similarities pose challenges for distinguishing them using satellite SAR imagery, making this a significant area of ongoing research.

Fishing vessels are used to harvest seafood and are essential to the global food supply chain. Monitoring and detecting fishing vessels is especially important due to the prevalence of illegal, unreported, and unregulated (IUU) fishing, which threatens marine biodiversity and the sustainability of global fish stocks, while costing legitimate fishermen and governments billions of dollars [18]. Detecting these vessels is challenging, particularly when they operate in remote areas or disable tracking systems. Their relatively small size and

erratic movement patterns further complicate identification using satellite SAR imagery. Passenger ships, including ferries and cruise liners, are designed to transport people and serve as key components of both public transportation and the tourism sector. Monitoring these ship types is essential for ensuring operational efficiency, environmental compliance, maritime safety, and the protection of marine ecosystems.

We considered five classification scenarios derived from combinations of four primary ship types using benchmark deep learning models, including ResNet, and ResNeXt variants[19], [20], DenseNet121 [21], EfficientNet [22], and Vision Transformers [23]. For brevity, only average results are reported. The framework, implemented in PyTorch, used Adam optimization with weighted cross-entropy loss to address class imbalance. Training employed a batch size of 16, learning rates between 0.0001–0.0005, and linear decay after five epochs without validation improvement. Ten-fold cross-validation ensured robustness, with 70% of data for training per fold.

Table I presents classification results, comparing model performance when trained on all the ships located in inshore or offshore areas. Inshore environments pose significant challenges due to the presence of land and infrastructure, which introduce additional scattering effects. These areas are characterized by cluttered backgrounds from static objects such as ports and buildings, making it difficult to distinguish ships from surrounding structures. The proximity to land also results in strong backscatter and land-sea boundary confusion, while small vessels with low radar cross-sections are particularly difficult to detect amid high clutter. Furthermore, multipath reflections and shadowing caused by coastal infrastructure can distort radar returns. Offshore areas, by contrast, present different challenges. The low contrast between ships and sea clutter, especially under rough conditions involving strong currents and waves, can produce scattering patterns and speckle noise that mimic or obscure ship signatures, particularly for small or low-profile vessels. Additionally, the motion of ships can introduce distortions such as azimuthal smearing, further complicating detection and classification.

To provide a more detailed analysis, classification results for ships in offshore and inshore areas are presented separately in Table II and Table III. In general, offshore scenarios exhibit better performance, with higher accuracy and precision. On the one hand, this can be attributed to factors as discussed above—namely, the presence of backscattering contributions from land and infrastructure in inshore areas, which can diminish the relative scattering from ships and hinder their identification, especially in lower-resolution imagery. However, this could also be considered indicative of the importance of ship wakes as discriminative features in identifying maritime platforms, since such features are not present inshore. Another contributing factor may also be the smaller number of samples available in inshore regions. This is reflected in the robustness of the offshore results (Table II), which show lower variation across the ten-fold cross-validation experiments, compared to higher fluctuations in the inshore results (Table III).

TABLE I
CLASSIFICATION RESULTS - INSHORE AND OFFSHORE SCENARIO

Categories	OA	AA	APr	AF1
Fishing, Other	87.6 \pm 2.9	78.2 \pm 5.5	79.0 \pm 4.8	77.6 \pm 4.5
Fishing, Cargo	88.5 \pm 3.3	84.7 \pm 4.9	87.9 \pm 3.5	85.8 \pm 4.4
Cargo, Tanker	75.4 \pm 1.6	65.7 \pm 2.1	76.4 \pm 4.0	66.7 \pm 2.5
Fishing, Cargo, Tanker	70.8 \pm 2.4	67.8 \pm 1.9	71.2 \pm 3.4	68.5 \pm 2.4
Fishing, Passenger, Cargo, Tanker	61.9 \pm 1.5	58.1 \pm 2.5	64.5 \pm 1.8	59.6 \pm 2.1

TABLE II
CLASSIFICATION RESULTS - OFFSHORE SCENARIO

Categories	OA	AA	APr	AF1
Fishing, Other	91.1 \pm 2.0	76.8 \pm 7.5	78.5 \pm 4.8	76.5 \pm 5.7
Fishing, Cargo	91.9 \pm 3.4	83.0 \pm 7.2	90.0 \pm 4.3	85.5 \pm 6.5
Cargo, Tanker	74.6 \pm 1.8	66.4 \pm 2.2	76.2 \pm 3.5	67.2 \pm 2.6
Fishing, Cargo, Tanker	70.7 \pm 3.1	66.4 \pm 2.0	72.2 \pm 4.3	68.0 \pm 2.2
Fishing, Passenger, Cargo, Tanker	61.6 \pm 1.5	54.7 \pm 3.6	63.1 \pm 2.0	56.6 \pm 3.2

TABLE III
CLASSIFICATION RESULTS - INSHORE SCENARIO

Categories	OA	AA	APr	AF1
Fishing, Other	78.9 \pm 6.8	75.9 \pm 4.0	77.5 \pm 5.1	75.2 \pm 5.6
Fishing, Cargo	79.2 \pm 5.6	78.3 \pm 4.8	79.3 \pm 5.4	77.7 \pm 5.3
Cargo, Tanker	75.0 \pm 9.1	60.7 \pm 11.6	66.5 \pm 17.3	60.2 \pm 10.3
Fishing, Cargo, Tanker	68.5 \pm 2.1	57.1 \pm 5.2	71.8 \pm 4.7	58.4 \pm 5.4
Fishing, Passenger, Cargo, Tanker	62.6 \pm 1.6	53.4 \pm 0.7	60.6 \pm 7.5	53.9 \pm 2.5

V. CONCLUSION

This paper introduces NASTaR, a dedicated dataset for ship-type classification, created by leveraging NovaSAR S-band imagery and AIS-derived labels. To build this dataset, we designed a detailed workflow to meticulously extract high-quality samples from SAR scenes and their corresponding AIS data. We also conducted comprehensive statistical analyses to demonstrate the dataset's versatility. To facilitate future research, NovaSARNet includes additional features such as ship-to-shore distance, inshore/offshore categorization, and a separate wake dataset for patches where ship wakes are visible, enabling further wake-related studies. The dataset's applicability was validated across prominent ship-type classification scenarios using benchmark deep learning models. Results show promising performance: over 60% accuracy for four major ship types, over 70% for a three-class scenario, more than 75% for distinguishing cargo from tanker ships, and over 87% for identifying fishing vessels. Future research can follow two main directions: Designing tailored deep learning architectures to improve benchmark results or further investigation of the impact of wake patterns on sea surface characteristics and their role in maritime activity monitoring.

ACKNOWLEDGMENT

The authors would like to thank Surrey Satellite Technology Ltd. (SSTL) and Airbus UK for the kind provision of NovaSAR image products. Copyright © 2025 SSTL.

REFERENCES

- W. G. Pichel, P. Clemente-Colon, C. C. Wackerman, and K. S. Friedman, "Ship and wake detection," in *Synthetic Aperture Radar Marine User's Manual*, C. R. Jackson and J. R. Apel, Eds. NOAA/NESDIS, U.S. Department of Commerce, 2004, ch. 12, pp. 277–303.
- K. Kamirul, O. Pappas, I. G. Rizaev, and A. Achim, "On the modelling of ship wakes in S-band SAR images and an application to ship identification," in *2024 IEEE Int. Geosci. Remote Sens. Symp. (IGARSS)*, 2024, pp. 10599–10603.
- C. M. Awais, M. Reggiannini, D. Moroni, and E. Salerno, "A survey on SAR ship classification using deep learning," *arXiv preprint arXiv:2503.11906*, 2025.
- C. Zhang, X. Zhang, G. Gao, H. Lang, G. Liu, C. Cao, Y. Song, Y. Guan, and Y. Dai, "Development and application of ship detection and classification datasets: A review," *IEEE Geosci. Remote Sens. Mag.*, 2024.
- X. Xing, K. Ji, H. Zou, W. Chen, and J. Sun, "Ship classification in TerraSAR-X images with feature space based sparse representation," *IEEE Geosci. Remote Sens. Lett.*, vol. 10, no. 6, pp. 1562–1566, 2013.
- L. Huang, B. Liu, B. Li, W. Guo, W. Yu, Z. Zhang, and W. Yu, "OpenSARShip: A dataset dedicated to Sentinel-1 ship interpretation," *IEEE J. Sel. Topics Appl. Earth Observ. Remote Sens.*, vol. 11, no. 1, pp. 195–208, 2017.
- B. Li, B. Liu, L. Huang, W. Guo, Z. Zhang, and W. Yu, "OpenSARShip 2.0: A large-volume dataset for deeper interpretation of ship targets in Sentinel-1 imagery," in *2017 SAR in Big Data Era: Models, Methods and Applications (BIGSARDATA)*. IEEE, 2017, pp. 1–5.
- F. Paolo, T.-t. T. Lin, R. Gupta, B. Goodman, N. Patel, D. Kuster, D. Kroodsma, and J. Dunnmon, "xView3-SAR: Detecting dark fishing activity using Synthetic Aperture Radar imagery," *Adv. Neural Inf. Process. Syst.*, vol. 35, pp. 37604–37616, 2022.
- X. Hou, W. Ao, Q. Song, J. Lai, H. Wang, and F. Xu, "FUSAR-Ship: Building a high-resolution SAR-AIS matchup dataset of Gaofen-3 for ship detection and recognition," *Sci. China Inf. Sci.*, vol. 63, no. 4, p. 140303, 2020.
- M. Ma, J. Chen, W. Liu, and W. Yang, "Ship classification and detection based on CNN using GF-3 SAR images," *Remote Sensing*, vol. 10, no. 12, p. 2043, 2018.
- C. Xu and X. Wang, "OpenSARWake: A large-scale SAR dataset for ship wake recognition with a feature refinement oriented detector," *IEEE Geosci. Remote Sens. Lett.*, vol. 21, pp. 1–5, 2024.
- I. G. Rizaev and A. Achim, "SynthwakeSAR: A synthetic SAR dataset for deep learning classification of ships at sea," *Remote Sensing*, vol. 14, no. 16, p. 3999, 2022.
- Y. Zhang, Z. Lei, H. Yu, and L. Zhuang, "Imbalanced high-resolution SAR ship recognition method based on a lightweight CNN," *IEEE Geosci. Remote Sens. Lett.*, vol. 19, pp. 1–5, 2021.
- C. Wang, J. Pei, S. Luo, W. Huo, Y. Huang, Y. Zhang, and J. Yang, "SAR ship target recognition via multiscale feature attention and adaptive-weighted classifier," *IEEE Geosci. Remote Sens. Lett.*, vol. 20, pp. 1–5, 2023.
- H. Zheng, Z. Hu, J. Liu, Y. Huang, and M. Zheng, "MetaBoost: A novel heterogeneous DCNNs ensemble network with two-stage filtration for SAR ship classification," *IEEE Geosci. Remote Sens. Lett.*, vol. 19, pp. 1–5, 2022.
- Danish Maritime Authority, "Historical AIS Data," Available online at <http://aisdata.ais.dk/>, accessed: 25 Nov. 2025.
- Natural Earth, "Natural earth vector 10m map," Available online at <https://www.naturalearthdata.com/>, accessed: 25 Nov. 2025.
- F. S. Paolo, D. Kroodsma, J. Raynor, T. Hochberg, P. Davis, J. Cleary, L. Marsaglia, S. Orofino, C. Thomas, and P. Halpin, "Satellite mapping reveals extensive industrial activity at sea," *Nature*, vol. 625, no. 7993, pp. 85–91, 2024.
- K. He, X. Zhang, S. Ren, and J. Sun, "Deep residual learning for image recognition," *arXiv preprint arXiv:1512.03385*, 2015.
- S. Xie, R. Girshick, P. Dollár, Z. Tu, and K. He, "Aggregated residual transformations for deep neural networks," *arXiv preprint arXiv:1611.05431*, 2016.
- G. Huang, Z. Liu, L. van der Maaten, and K. Q. Weinberger, "Densely connected convolutional networks," in *Proceedings of the IEEE Conference on Computer Vision and Pattern Recognition*, 2017.
- M. Tan and Q. Le, "Efficientnetv2: Smaller models and faster training," in *International conference on machine learning*. PMLR, 2021, pp. 10096–10106.
- K. Wu, J. Zhang, H. Peng, M. Liu, B. Xiao, J. Fu, and L. Yuan, "TinyViT: Fast pretraining distillation for small vision transformers," in *European conference on computer vision (ECCV)*, 2022.